

## Tri- and tetra-substituted naphthalene diimides as potent G-quadruplex ligands

Francisco Cuenca,<sup>a</sup> Olga Greciano,<sup>a</sup> Mekala Gunaratnam,<sup>a</sup> Shozeb Haider,<sup>a</sup> Deeksha Munnur,<sup>a</sup> Rupesh Nanjunda,<sup>b</sup> W. David Wilson<sup>b</sup> and Stephen Neidle<sup>a,\*</sup>

<sup>a</sup>CRUK Biomolecular Structure Group, The School of Pharmacy, University of London, 29/39 Brunswick Square, London WC1N 1AX, UK

<sup>b</sup>Department of Chemistry, Georgia State University, Atlanta, GA 30303, USA

Received 20 December 2007; revised 10 January 2008; accepted 14 January 2008

Available online 18 January 2008

**Abstract**—A series of tri- and tetra-substituted naphthalene diimides have been designed and synthesized. Several compounds show exceptional affinity for telomeric G-quadruplex DNA in classical and competition FRET assays and SPR studies. They inhibit telomerase in the TRAP assay, and show potent senescence-based short-term anti-proliferative effects on MCF7 and A549 cancer cell lines, and localize in the nucleus and particularly the nucleolus of MCF7 cells.

© 2008 Elsevier Ltd. All rights reserved.

Telomeres are highly specialized DNA-protein structures at the ends of eukaryotic chromosomes<sup>1</sup> whose integrity is required for the cell to avoid end-to-end fusions and recombination.<sup>2</sup> Telomere length progressively shortens in somatic cells with successive rounds of cell division, leading eventually to senescence and apoptosis. In contrast telomere length is maintained in cancer cells and is a major factor in immortalization and tumorigenesis.<sup>3</sup> The reverse transcriptase enzyme telomerase is over-expressed in ca 80–85% of cancer cell types<sup>4</sup> where its ability to catalyze the synthesis of telomeric DNA repeats is responsible for telomere homeostasis. Inhibition of telomerase induces cell senescence and cell death in cancer cells and it is a validated target for cancer therapeutics.<sup>5</sup>

One approach to telomerase inhibition involves sequestering its substrate, single-stranded telomeric DNA, by inducing it to form G-quadruplex (G4) structures.<sup>6</sup> Induction of a G-quadruplex conformation can be achieved by small-molecule ligands; a large number have been reported,<sup>7</sup> although none as yet have reached the clinic. It has been shown that the induction of G4-ligand

complexes at the 3'-single-strand telomeric DNA overhang displaces telomere-associated proteins such as hPOT1 and telomerase.<sup>8</sup> This unmasking of the 3'-overhang invokes a rapid DNA damage response, which rapidly leads to selective cell death and anti-tumour activity *in vivo*.<sup>9</sup>

A number of naphthalene imide and diimide (ND) monomer and dimer derivatives bind to duplex DNA.<sup>10</sup> Several show *in vivo* anti-cancer activity and two (Amonafide and Elinafide) have been evaluated in anti-cancer clinical trials in humans,<sup>11</sup> although they have not progressed due to toxicity combined with limited activity. A series of disubstituted NDs have been screened as G4 ligands but showed only low affinity.<sup>12</sup> We hypothesized that the planarity of the ND moiety would nevertheless be an interesting starting point for the development of more complex ligands since recent chemical developments<sup>13</sup> enabled us to envisage a synthetic route to tetra-substituted analogues, which we argued, would possess high affinity for G4s such as the parallel telomeric G4 structure which possesses four targetable grooves.<sup>14</sup> This supposition was supported by molecular modelling studies<sup>15</sup> (Fig. 1), and more recently, by crystallographic analyses on several G4-ND complexes.<sup>16</sup> Furthermore, the synthetic route allows the introduction to the ND core of up to three different side chains, which in principle can be exploited to produce ligand diversity that may discriminate between

**Keywords:** G-quadruplex; Telomere; Telomerase inhibition.

\* Corresponding author. Tel.: +44 207 753 5969; fax: +44 207 753 5970; e-mail: [bmcl@pharmacy.ac.uk](mailto:bmcl@pharmacy.ac.uk)

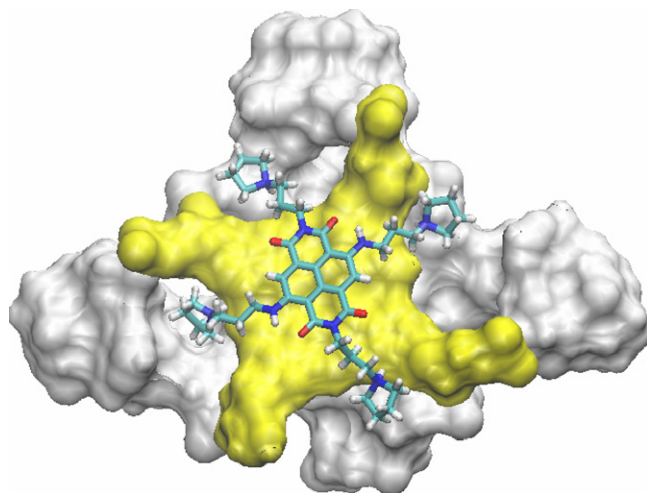


**Figure 1.** Molecular model of **11** bound to the 5' face of the human intramolecular G4 structure (van der Waals surface coloured grey with the 5' G-tetrad highlighted in yellow), after 5 ns of molecular dynamics simulation. The MM-PBSA-calculated binding energy is  $-60.6 \text{ kcal mole}^{-1}$ , compared to  $-39.4 \text{ kcal mole}^{-1}$  for the acridine ligand BRACO19.<sup>8a,9a</sup>

different types of G-quadruplexes. This feature will be reported elsewhere.

We report here on a library of tri- and tetra-substituted ND analogues accessible from commercially available amines. The differences in the amines have provided diversity in the library, enabling exploration of the effects of differing end groups, side-chain lengths, and to some extent, non-equivalent side chains.

The synthesis of the final compounds (Table 1) was conducted in one or two steps from the key intermediates 2,6-dibromo-1,4,5,8-naphthalene tetra-carboxylic acid dianhydride (**1**) or 2,6-dichloro-1,4,5,8-naphthalene tetra-carboxylic acid dianhydride (**2**) (Scheme 1). The tetra-substituted analogues containing four equal side chains could be synthesized from either **1** or **2** using neat amine as a solvent and heating at  $150 \text{ }^\circ\text{C}$  for 10 min in a microwave. The more economical dibromo compound **1** was preferentially used.

It was found that the tri-substituted (and occasionally di-substituted) analogues were regularly obtained as by-products in the reactions using **1**. We hypothesized that the occurrence of these sub-products was due to radical debromination of the starting materials or intermediates caused by traces of DBI used in a previous synthetic step.<sup>13</sup> Although initially unwanted, this side reaction proved to be useful as the tri-substituted analogues together with the targeted compounds were consistently isolated from the crude reaction product using HPLC.<sup>17</sup>

It has been reported that the substitution reaction at the anhydride groups of compound **1** can be successfully decoupled from the reactions at the bromines.<sup>18</sup> In our hands, however, this reaction did not show the expected selectivity and complex mixtures were obtained. For this

reason compound **2** was used for the synthesis of compounds **23** and **24** where two different side chains were used. For this two-step synthesis compound **2** was treated with the first amine in acetic acid and subsequently with the second amine for the substitution at the chlorines. The disubstituted compounds **25** and **26** previously reported,<sup>10a</sup> were synthesized using commercially available naphthalene dianhydride and the correspondent amine.

The initial assessment of the DNA stabilization ability of the compounds was done using a FRET melting assay.<sup>19</sup> We used two different DNA sequences, a human telomeric G4 and a self-complementary duplex DNA hairpin. We also ran FRET competition experiments<sup>20</sup> in which affinity for the G4 sequence is evaluated in the presence of increasing concentrations of duplex DNA. Together, these experiments enabled us to assess the selectivity of the ligands for G4 versus duplex DNA (Table 1 and Fig. 2).

$\Delta T_m$  values are given at ligand concentrations of  $0.5 \mu\text{M}$  since a high level of G4 DNA stabilization was observed for a number of the ligands. For example, the  $\Delta T_m$  of  $35.2 \text{ }^\circ\text{C}$  for compound **7** contrasts with the behaviour of the tri-substituted acridine BRACO19,<sup>8a,9a</sup> which produced an equivalent  $\Delta T_m$  value at a concentration of  $2.5 \mu\text{M}$ . Overall, the tetra-substituted ligands (4-ND) show superior G4 stabilization compared to the tri-substituted ones (3-ND) and these in turn are superior to the di-substituted counterparts (2-ND). Compounds with four side chains have higher stabilizing ability regardless of the overall number of cationic charges as the effect is observed for compounds **15/16**, **17/18** and **21/22**, which are uncharged or weakly cationic at pH 7.4 (the pH at which the FRET experiments were performed). Compounds **3**, **7** and **11** and **4**, **8** and **12** have the highest  $\Delta T_m$  within the 4-ND and 3-ND series, respectively. They all have side chains of the same length (3 carbons) and similar end groups (tertiary amines, protonated at pH 7.4). Their counterparts with shorter side chains, **5**, **9** and **13** and **6**, **10** and **14**, respectively, all give lower  $\Delta T_m$  values. Side chains of at least three carbon atoms are necessary to deliver the end groups to the grooves of the G4, as the molecular modelling suggests (Fig. 1). Substitution of the tertiary amines for morpholino groups in compounds **15**, **16**, **17** and **18** reduces the  $\Delta T_m$ , as observed previously in other series of G4 ligands.<sup>21</sup> However, these morpholino and also the hydroxyl analogues **21** and **22** all show a high level of G4 stabilization. With the notable exception of telomestatin, to our knowledge, very few other neutral ligands show a similar degree of G4 affinity.<sup>7</sup> The 2-substituted NDs examined here (compounds **25** and **26**), show poor G4 affinity, in accord with earlier observations.<sup>12</sup>

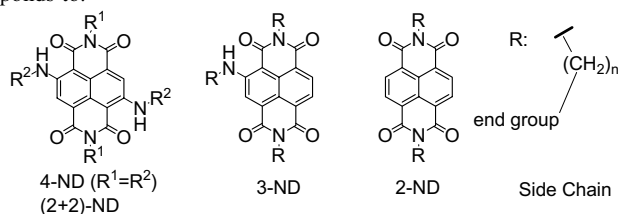
Most NDs reported here showed at least some interaction with duplex DNA. Compounds **21** and **22** however, slightly destabilized the duplex sequence. With the exception of the pair of compounds **5/6**, the tri-substituted NDs are more effective binders to the duplex DNA than the tetra-substituted analogues, probably be-

**Table 1.** ND compounds synthesized and the results of FRET melting studies, where  $\Delta T_m$  values are estimated as the mid-points of the melting transition for Q (human G4 quadruplex) and d (a duplex DNA sequence)

Compound	Core <sup>a</sup>	Side chain		FRET-Q <sup>d</sup> (°C)		FRET-d <sup>c</sup> (°C)	
		<i>n</i> <sup>b</sup>	End group <sup>c</sup>	$\Delta T_m$ (0.5 $\mu$ M)			
3	4-ND	3	DMA	33.2	4.5		
4	3-ND	3	DMA	26.5	12.5		
5	4-ND	2	DMA	28	7.5		
6	3-ND	2	DMA	17.2	4.2		
7	4-ND	3	DEA	35.2	4.2		
8	3-ND	3	DEA	26.2	11.5		
9	4-ND	2	DEA	30	4		
10	3-ND	2	DEA	21	5		
11	4-ND	3	Pyrr	34.5	2		
12	3-ND	3	Pyrr	28.2	10.7		
13	4-ND	2	Pyrr	29.7	3.5		
14	3-ND	2	Pyrr	21.2	6.5		
15	4-ND	3	Mor	20.5	3.7		
16	3-ND	3	Mor	10.2	3.2		
17	4-ND	2	Mor	13.7	3		
18	3-ND	2	Mor	6.2	3		
19	4-ND	2	Pip	27.5	2.2		
20	3-ND	2	Pip	17.5	4.7		
21	4-ND	5	OH	14.2	-0.5		
22	3-ND	5	OH	10.5	-0.5		
23	(2 + 2)-ND	R <sup>1</sup> : 3 R <sup>2</sup> : 2	R <sup>1</sup> : DMA R <sup>2</sup> : Pip	27.7	0.2		
24	(2 + 2)-ND	R <sup>1</sup> : 3 R <sup>2</sup> : 3	R <sup>1</sup> : DMA R <sup>2</sup> : OH	23.7	3.5		
25	2-ND	3	DMA	5.2	2.7		
26	2-ND	2	DMA	3.2	1		

Values are the means of two determinations.

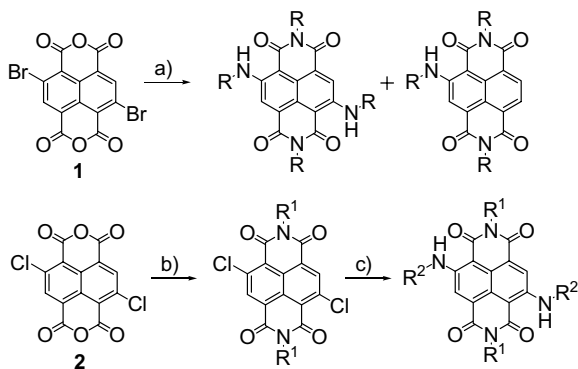
<sup>a</sup> Nomenclature used in the table corresponds to:



<sup>b</sup> Number of carbons in the side chain linker.

<sup>c</sup> DMA, dimethylamine; DEA, diethylamine; Pyrr, pyrrolidine; Mor, morpholine; Pip, piperidine; OH, hydroxyl.

<sup>d</sup> See supplementary data for materials and methods.



**Scheme 1.** Synthesis of tri- and tetra-substituted naphthalene diimide analogues. Reactions and conditions: (a) Amine  $\text{RNH}_2$ , 150 °C, 10 min, MW; (b) Amine  $\text{R}^1\text{NH}_2$ , acetic acid, 120 °C, 10 min, MW; (c) Amine  $\text{R}^2\text{NH}_2$ , 150 °C, 10 min, MW.

cause of steric reasons. Compound **23**, with mixed-length side chains, has the highest G4/duplex selectivity of all while being a strong G4 binder. The reason for this selectivity is not understood and further investigation is underway.

The 4-NDs showed the best selectivity for G4 versus duplex DNA in the competition experiments, followed by the 3-NDs and then the 2-NDs (Fig. 2). Compounds **15**, **16** and **18**, and particularly the hydroxyl compounds **21** and **22**, stood out as the most G4 selective compounds within the series.

Biosensor-SPR binding studies were conducted on a representative set of NDs with an immobilized human G4 model sequence as previously described.<sup>22,23</sup> A table of binding ( $K_a$ ) and dissociation rate constants ( $k_d$ ) is in-

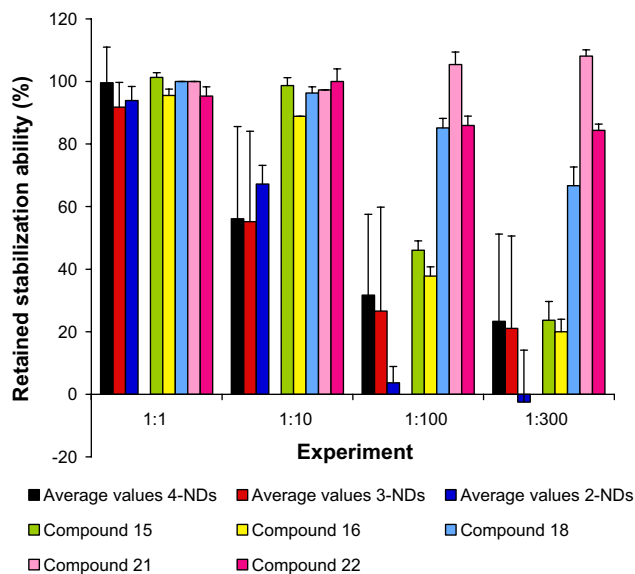


**Figure 2.** Competition FRET results. Y-axis represents the G4 stabilization ability of the compounds when in presence of a duplex DNA competitor (in the ratios depicted in X-axis, G4:duplex) normalized using 100% for the experiment without duplex competitor. See Supplementary Data for a full description of methods and results.

cluded in the Supplementary Data. The sensorgrams for all compounds reach a steady-state plateau between 100 and 200 s after initiation of compound injection. The steady-state RU values were determined by averaging in the steady-state region and were plotted versus the free compound concentration in the flow solution for determination of the  $K_a$  values. Sensorgrams for binding of 4-ND **7** and 2-ND **25** are compared in Figure 3 and a sensorgram plus a binding plot for compound **8** are shown in the Supplementary Data. Although both compounds in Figure 3 bind to the G4, significant differences can be seen in the sensorgrams, especially in the dissociation rate, which is much slower for **7** than for **25**. Because of surface absorption of the compounds in the initial period of injection, it is not possible to quantitatively determine their association kinetics constants. For the dissociation reaction, however, it is clear that the 2-ND dissociates in the first few sec of buffer flow while the apparent half-life for dissociation of the 4-ND is approximately 35 s. The 3-NDs have  $k_d$  rates that are more similar to the 4-NDs than the 2-NDs. An exception is compound **22**, which has considerably weaker binding and faster dissociation rates from the G4 than

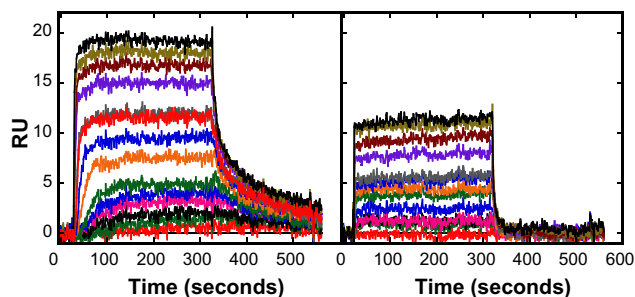


**Figure 3.** SPR sensorgrams for compounds **7** and **25**.

**7** has a single very strong binding site with  $K_a$  of  $3.1 \times 10^7 \text{ M}^{-1}$  and a weaker secondary site with a  $K$  ca 50× weaker. The binding of **25** is almost 10× lower with  $K_a$  of  $4.5 \times 10^6 \text{ M}^{-1}$  and a still weaker second binding site. In agreement with the  $T_m$  studies, compound **3** has a  $K_a$  that is similar to but slightly weaker than that for **7** while binding of **5** is somewhat weaker than for **3**. These results show that the 4-NDs are among the strongest G4 binding compounds found to date.<sup>23</sup> In agreement with its  $T_m$ , **5**, with a two-methylene linker, is the weakest binding 4-ND, with the highest  $k_d$  while **7**, with three methylenes, has the highest  $K_a$  and lowest  $k_d$ .

A group of ligands representative of the diversity in the library were also evaluated as telomerase inhibitors using a modified TRAP assay<sup>24</sup> (Table 2). Values of  $EC_{50}$  between 12 and 28  $\mu\text{M}$  were obtained with the exception of compound **17** ( $>50 \mu\text{M}$ ). No simple correlation between the FRET and TRAP data is evident but compound **17** is the poorest ligand in the FRET assay in the group. Two established G4 ligands, BRACO19<sup>8a,9a</sup> and TMPyP4<sup>25</sup>, were also evaluated in the TRAP assay and the  $EC_{50}$  values are consistent with a recent report using a direct telomerase assay.<sup>26</sup> The ND compounds have potencies of the same order as BRACO19 or TMPyP4. Note that these values are not comparable with most previously published TRAP assay results, which have not taken into account the need to remove ligand from the second (PCR) step of the assay. These results are more comparable with recent direct telomerase assay data.<sup>26</sup>

The ability of the compounds to produce short-term cell growth inhibition against two cancer cell lines (MCF7 and A549, both of which express telomerase), and a normal human fibroblast line (WI38) was assessed using the sulforhodamine B (SRB) assay. The compounds as a class show potent cell growth arrest, especially in the cancer cell lines (Table 3), although there is wide variation in behaviour, with the most potent compounds such as **4**, **5**, **12–14** having  $IC_{50}$  values of 5–10 nM. The MCF7 cell line is consistently the most sensitive. In general, potency correlates with high G4 affinity. This is especially evident for the morpholino compounds **16–18**, which are relatively non-toxic in the three cell lines (although the cell uptake of these compounds may be low—see below).

**Table 2.** TRAP telomerase inhibition results<sup>a</sup>

Compound	TRAP $EC_{50}$ ( $\mu\text{M}$ )
<b>3</b>	25
<b>4</b>	17
<b>7</b>	21.3
<b>8</b>	27.9
<b>11</b>	21
<b>13</b>	12.3
<b>17</b>	$>50^b$
BRACO19	7.9
TMPyP4	16.4

<sup>a</sup> Values are the averages of two independent experiments, apart from **13**.

<sup>b</sup> No inhibition observed at concentrations of up to 50  $\mu\text{M}$ .

**Table 3.** SRB and senescence data for the ND compounds

Compound	IC <sub>50</sub> (nM) <sup>a</sup>			Senescence (% of cells) after 1 wk treatment
	MCF7	A549	WI38	
3	104.7	28.7	292.3	35.0 ± 3 (at 70 nM)
4	5.4	13.3	42.8	n.a. <sup>b</sup>
5	9.2	15.3	40.1	n.a.
6	18.5	25.1	137.5	n.a.
7	18	10.7	86.7	n.a.
8	17.9	48	83.7	35 ± 3 (at 15 nM)
9	219	273.9	971.9	n.a.
10	164.4	144	466.8	n.a.
11	81.3	115.3	167.2	45 ± 6 (at 75 nM)
12	10.5	96	62.6	n.a.
13	10.2	13.6	63.4	n.a.
14	11	18.3	63.9	n.a.
15	437	1190	965	n.a.
16	800	1320	1220	n.a.
17	6700	>10000	>10000	51 ± 3 (at 3.5 μM)
18	1610	2750	8500	n.a.
19	295.7	204.5	1460	n.a.
20	128.9	145.6	438.9	n.a.
21	8300	>10000	>10000	n.a.
22	9200	>10000	>10000	n.a.
23	26.9	57.1	57.7	n.a.
24	287.7	1700	10000	n.a.
25	135.2	113.8	210.9	n.a.
26	118.9	99.1	171.1	n.a.

<sup>a</sup> Standard deviations omitted for clarity.

<sup>b</sup> n.a., not available.

The observation of cellular senescence as a result of G4 ligand action at telomeres is well-documented.<sup>8,27</sup> The senescence phenotype was investigated in MCF7 cells treated for one week with sub-cytotoxic concentrations for a few compounds.<sup>28</sup> All those evaluated showed a significant increase in the percentage of senescence cells after treatment (Table 3), surprisingly even for those with higher IC<sub>50</sub> values. We conclude that the senescence effects are consistent with telomerase inhibition and that the ability of NDs to selectively kill cancer cells is at least in part a consequence of telomere targeting and telomerase uncapping effects.

The ND-3 and ND-4 compounds reported here show profound fluorescence. This facilitated localization of a selected group of compounds within MCF7 cells using confocal microscopy. Compounds 3, 8 and 11 localize exclusively in the nucleus following 30 min exposure at a concentration of 0.5 μM (Figure 4-1). For 17, less intense and more widespread distributed fluorescence was observed upon cell exposure even up to a concentration of 50 μM (Figure 4-2). This may partially account for the lower toxicity of 17 and the other morpholino analogues 15, 16 and 18. The compounds that concentrated in the nucleus showed preference for the nucleolus (Figure 4-3). It may be significant for their action that telomerase trafficking is associated with the nucleolus.<sup>29</sup>

We have shown here that a number of tri- and tetra-substituted NDs are exceptional G4 binding agents, with Δ*T*<sub>m</sub> values for the human intramolecular G4 that are at least twofold greater than that of the acridine compound

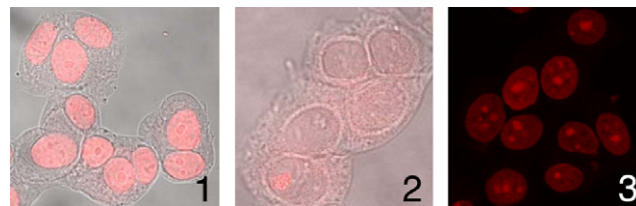


**Figure 4.** Cell uptake detection using fluorescence confocal microscopy. (1) Transmission/fluorescence composite image of 11 localized in the nucleus of MCF7 cells after 30 min exposure at 0.5 μM; (2) non-specific and low uptake of 17 after 30 min exposure at 50 μM; (3) Image of 3 localized in the nucleolus after 30 min at 0.5 μM.

BRACO19, and significantly greater than the effects produced by TMPyP4 and telomestatin (data not shown). Whether this is a significant factor in the potency shown by a number of these NDs in inhibiting cancer cell growth, remains to be demonstrated. The flexible synthetic route described here may yield new ligands with improved G4/duplex selectivity, which will help to further define their mechanism of action. The crystal structures of G4-ND complexes<sup>16</sup> may also facilitate future structure-based design studies.

### Acknowledgments

We are grateful to CRUK, EU FP6 (Molecular Cancer Medicine) and the Heptagon Fund for support, and Drs. J.-L. Mergny and A. de Cian for preliminary *T*<sub>m</sub> experiments and much useful discussion.

### Supplementary data

Supplementary data for this article can be found online at, doi:10.1016/j.bmcl.2008.01.050.

### References and notes

- McEachern, M. J.; Krauskopf, A.; Blackburn, E. H. *Ann. Rev. Genetics* **2000**, *34*, 331.
- Smogorzewska, A.; De Lange, T. *Annu. Rev. Biochem.* **2004**, *73*, 177.
- Hahn, W. C.; Counter, C. M.; Lundberg, A. S.; Beijersbergen, R. L.; Brooks, M. W.; Weinberg, R. A. *Nature* **1999**, *400*, 464.
- Kim, N. W.; Piatyszek, M. A.; Prowse, K. R.; Harley, C. B.; West, M. D.; Ho, P. L. C.; Coviello, G. M.; Wright, W. E.; Shay, J. W. *Science* **1994**, *266*, 2011.
- (a) Hahn, W. C.; Stewart, S. A.; Brooks, M. W.; York, S. G.; Eaton, E.; Kurachi, A.; Beijersbergen, R. L.; Knoll, J. H. M.; Meyerson, M.; Weinberg, R. A. *Nat. Med.* **1999**, *5*, 1164; (b) Shay, J. W.; Wright, W. E. *Nat. Rev. Drug Discov.* **2006**, *5*, 577.
- (a) Zahler, A. M.; Williamson, J. R.; Cech, T. R.; Prescott, D. M. *Nature* **1991**, *350*, 718; (b) Sun, D.; Thompson, B.; Cathers, B. E.; Salazar, M.; Kerwin, S. M.; Trent, J. O.; Jenkins, T. C.; Neidle, S.; Hurley, L. H. *J. Med. Chem.* **1997**, *40*, 2113; (c) Oganessian, L.; Bryan, T. M. *Bioessays* **2007**, *25*, 155.
- Comprehensively reviewed in: De Cian, A.; Lacroix, L.; Douarre, C.; Temime-Smaali, N.; Trentesaux, C.; Riou, J.-F.; Mergny, J.-L. *Biochimie*. **2007**, *in press*.

8. (a) Gunaratnam, M.; Greciano, O.; Martins, C.; Reszka, A. P.; Schultes, C. M.; Morjani, H.; Riou, J.-F.; Neidle, S. *Biochem. Pharmacol.* **2007**, *74*, 679; (b) Brassart, B.; Gomez, D.; De Cian, A.; Paterski, R.; Montagnac, A.; Qui, K. H.; Temime-Smaali, N.; Trentesaux, C.; Mergny, J.-L.; Gueritte, F.; Riou, J.-F. *Mol. Pharmacol.* **2007**, *72*, 631.
9. (a) Burger, A. M.; Dai, F.; Schultes, C. M.; Reszka, A. P.; Moore, M. J.; Double, J. A.; Neidle, S. *Cancer Res.* **2005**, *65*, 1489; (b) Phatak, P.; Cookson, J. C.; Dai, F.; Smith, V.; Gartenhaus, R. B.; Stevens, M. F. G.; Burger, A. M. *Brit. J. Cancer* **2007**, *96*, 1223.
10. See for example: (a) Yen, S.-F.; Gabbay, E. J.; Wilson, W. D. *Biochemistry* **1982**, *21*, 2070; (b) Tanious, F. A.; Yen, S. F.; Wilson, W. D. *Biochemistry* **1991**, *30*, 1813; (c) Lee, J.; Guelev, V.; Sorey, S.; Hoffman, D. W.; Iverson, B. L. *J. Amer. Chem. Soc.* **2004**, *126*, 14036.
11. (a) Brana, M. F.; Ramos, A. *Curr. Med. Chem. Anticancer Agents* **2001**, *1*, 237; (b) Van Quaquebeke, E.; Mahieu, T.; Dumont, P.; Dewelle, J.; Ribaucour, F.; Simon, G.; Sauvage, S.; Gaussin, J.-F.; Tuti, J.; El Yazidi, M.; Van Vynck, F.; Mijatovic, T.; Lefranc, F.; Darro, F.; Kiss, R. *J. Med. Chem.* **2007**, *50*, 4122.
12. Sissi, C.; Lucatello, L.; Paul, K. A.; Maloney, D. J.; Boxer, M. B.; Camarasa, M. V.; Pezzoni, G.; Menta, E.; Palumbo, M. *Bioorg. Med. Chem.* **2007**, *15*, 555.
13. Thalacker, C.; Roger, C.; Wurthner, F. *J. Org. Chem.* **2006**, *71*, 8098.
14. Parkinson, G. N.; Lee, M. P.; Neidle, S. *Nature* **2002**, *417*, 876.
15. The crystal structure of the 22-mer intramolecular parallel-stranded human telomeric G4 DNA (PDB id 1KFI) was used to model interactions with ND ligands. Ligand structures were randomly positioned over the 5' terminal G-tetrad. A simulated annealing docking protocol located and then optimized ligand placements, followed by 5–10 ns molecular dynamics simulations. The MM-PBSA method was used to calculate intermolecular interaction energies.
16. Crystal structures of intra- and intermolecular G4 ND ligand complexes have been solved in this laboratory, and will be reported separately. All show G4s with parallel topology, in accord with the structural model shown here.
17. Synthesis and analytical data for compounds **3** and **4**. Data on other compounds are available as [Supplementary Data](#). Compound **1** (100 mg, 0.234 mmol) was suspended in *N,N*-dimethyl-1,3-propanediamine (0.5 ml) in a microwave reaction vessel, then flushed with nitrogen, sealed and treated at 150 °C for 10 min in the microwave. The amine was then evaporated off under high vacuum. The crude mixture was purified by HPLC to obtain **3** and **4** as a blue and an orange solid, respectively. Yield **3** (23.1 mg, 0.036 mmol, 15.5%), **4** (12.6 mg, 0.024 mmol, 10.0%). Analytical data **3**: <sup>1</sup>H NMR (CDCl<sub>3</sub>) δ: 1.90 (5q, 4H, *J* = 7.4 Hz), 1.94 (5q, 4H, *J* = 7.0 Hz), 2.26 (s, 12H), 2.27 (s, 12H), 2.44 (m, 8H), 3.57 (m, 4H), 4.22 (m, 4H), 8.16 (s, 2H), 9.41 (t, 2H, *J* = 5.1 Hz); <sup>13</sup>C NMR (CDCl<sub>3</sub>) δ: 26.10 (2 × CH<sub>2</sub>), 27.51 (2 × CH<sub>2</sub>), 38.71 (2 × CH<sub>2</sub>), 41.25 (2 × CH<sub>2</sub>), 45.41 (4 × CH<sub>3</sub>), 45.52 (4 × CH<sub>3</sub>), 56.99 (2 × CH<sub>2</sub>), 57.32 (2 × CH<sub>2</sub>), 101.93 (2 × C), 118.37 (2 × CH), 121.17 (2 × C), 125.79 (2 × C), 149.19 (2 × C), 163.05 (2 × C=O), 166.12 (2 × C=O); HRMS (ES<sup>+</sup>) calcd C<sub>34</sub>H<sub>52</sub>N<sub>8</sub>O<sub>4</sub> [M+H]<sup>+</sup> 637.4190. Found: 637.4199. Analytical data **4**: <sup>1</sup>H NMR (CDCl<sub>3</sub>) δ: 1.90 (5q, 2H, *J* = 7.2 Hz), 1.91 (5q, 2H, *J* = 7.5 Hz), 1.96 (5q, 2H, *J* = 6.9 Hz), 2.24 (s, 6H), 2.26 (s, 6H), 2.27 (s, 6H), 2.41–2.47 (m, 6H), 3.67 (m, 2H), 4.23 (m, 4H), 8.27 (s, 1H), 8.32 (d, 1H, *J* = 7.8 Hz), 8.63 (d, 1H, *J* = 7.8 Hz), 10.21 (t, 1H, *J* = 5.5 Hz); <sup>13</sup>C NMR (CDCl<sub>3</sub>) δ: 26.00 (CH<sub>2</sub>), 26.08 (CH<sub>2</sub>), 27.48 (CH<sub>2</sub>), 38.68 (CH<sub>2</sub>), 39.25 (CH<sub>2</sub>), 41.32 (CH<sub>2</sub>), 45.36 (2 × CH<sub>3</sub>), 45.41 (2 × CH<sub>3</sub>), 45.48 (2 × CH<sub>3</sub>), 56.65 (CH<sub>2</sub>), 57.22 (CH<sub>2</sub>), 57.31 (CH<sub>2</sub>), 99.88 (C), 119.42 (C), 119.97 (CH), 123.56 (C), 124.36 (CH), 126.18 (C), 127.93 (C), 129.57 (C), 131.22 (CH), 152.44 (C), 162.99 (C=O), 163.05 (C=O), 163.39 (C=O), 166.12 (C=O); HRMS (ES<sup>+</sup>) calcd C<sub>29</sub>H<sub>40</sub>N<sub>6</sub>O<sub>4</sub> [M+H]<sup>+</sup> 537.3189. Found: 537.3217.
18. Jones, B. A.; Facchetti, A.; Marks, T. J.; Wasielewski, M. R. *Chem. Mater.* **2007**, *19*, 2703.
19. The FRET DNA melting assay was performed as described previously Schultes, C. M.; Guyen, B.; Cuesta, J.; Neidle, S. *Bioorg. Med. Chem. Lett.* **2004**, *14*, 4347. The full protocol is given in the [Supplementary Data](#). Tagged DNA sequences were used, 5'-FAM-d(GGG[TTAGGG]<sub>3</sub>)-TAMRA-3' for the G4 and 5'-FAM-dTATAGCTATA-HEG-TATAGC-TATA-TAMRA-3' (HEG linker: [(-CH<sub>2</sub>-CH<sub>2</sub>-O)<sub>6</sub>]) for the duplex experiment. The assay employs 96-well plates and was processed with a DNA Engine Opticon instrument (MJ Research).
20. Assay performed as described above for the G4 experiment but with addition of varying concentrations of calf thymus DNA (Sigma-Aldrich, UK). Moorhouse, A. D.; Santos, A. M.; Gunaratnam, M.; Moore, M.; Neidle, S.; Moses, J. E. *J. Am. Chem. Soc.* **2006**, *128*, 15972.
21. For example: Harrison, R. J.; Gowan, S. M.; Kelland, L. R.; Neidle, S. *Bioorg. Med. Chem. Lett.* **1999**, *9*, 2463.
22. Moore, M. J.; Schultes, C. M.; Cuesta, J.; Cuenca, F.; Gunaratnam, M.; Tanious, F. A.; Wilson, W. D.; Neidle, S. *J. Med. Chem.* **2006**, *49*, 582.
23. White, E. W.; Tanious, F.; Ismail, M. A.; Reszka, A. P.; Neidle, S.; Boykin, D. W.; Wilson, W. D. *Biophys. Chem.* **2007**, *126*, 140.
24. This TRAP assay includes a ligand removal step between elongation and PCR to avoid ligand interference effects (Reed et al., to be published).
25. Shi, D. F.; Wheelhouse, R. T.; Sun, D.; Hurley, L. H. *J. Med. Chem.* **2001**, *44*, 4509.
26. De Cian, A.; Cristofari, G.; Reichenbach, P.; De Lemos, E.; Mondchaud, D.; Teulade-Fichou, M. P.; Shin-Ya, K.; Lacroix, L.; Lingner, J.; Mergny, J.-L. *Proc. Natl. Acad. Sci. U.S.A.* **2007**, *104*, 17347.
27. Riou, J.-F.; Guittat, L.; Mailliet, P.; Laoui, A.; Renou, E.; Petitgenet, O.; Megnin-Chanet, F.; Hélène, C.; Mergny, J.-L. *Proc. Natl. Acad. Sci. U.S.A.* **2002**, *99*, 2672.
28. 1 × 10<sup>5</sup> cells per well were cultivated in 2 ml of medium plus compound in 96-well plates (Fisher Scientific, UK). After 24 h the cells were stained for senescence with a β-galactosidase kit (Cell Signalling Technology). Senescent cells, stained blue, were quantified by microscopy.
29. Tomlinson, R. L.; Ziegler, T. D.; Supakordej, T.; Terns, R. M.; Terns, M. P. *Mol. Cell. Biol.* **2006**, *17*, 955.